

Depletion of Nonlinearity in Magnetohydrodynamic Turbulence: Insights from Analysis and Simulations

J. D. Gibbon¹, A. Gupta², G. Krstulovic³, R. Pandit⁴, H.

Politano⁵, Y. Ponty³, A. Pouquet^{6,7}, G. Sahoo², and J. Stawarz⁷

¹*Department of Mathematics, Imperial College London, London SW7 2AZ, UK.*

²*Department of Physics, University of Rome ‘Tor Vergata’, 00133 Roma, Italy.*

³*Laboratoire Lagrange, Université Côte d’Azur, Observatoire de la Côte d’Azur, CNRS, Blvd de l’Observatoire, CS 34229, 06304 Nice cedex 4, France*

⁴*Centre for Condensed Matter Theory, Indian Institute of Science, Bangalore, 560 012, India.*

⁵*Laboratoire Dieudonné, Université de Nice Sophia-Antipolis, France.*

⁶*National Center for Atmospheric Research,*

P.O. Box 3000, Boulder, CO 80307, USA.

⁷*Laboratory for Atmospheric and Space Physics,*

University of Colorado, Boulder, CO 80303, USA.

We build on recent developments in the study of fluid turbulence [Gibbon *et al.* Nonlinearity 27, 2605 (2014)] to define suitably scaled, order- m moments, D_m^\pm , of $\omega^\pm = \omega \pm \mathbf{j}$, where ω and \mathbf{j} are, respectively, the vorticity and current density in three-dimensional magnetohydrodynamics (MHD). We show by mathematical analysis, for unit magnetic Prandtl number P_M , how these moments can be used to identify three possible regimes for solutions of the MHD equations; these regimes are specified by inequalities for D_m^\pm and D_1^\pm . We then compare our mathematical results with those from our direct numerical simulations (DNSs) and thus demonstrate that 3D MHD turbulence is like its fluid-turbulence counterpart insofar as all solutions, which we have investigated, remain in *only one of these regimes*; this regime has depleted nonlinearity. We examine the implications of our results for the exponents q^\pm that characterize the power-law dependences of the energy spectra $\mathcal{E}^\pm(k)$ on the wave number k , in the inertial range of scales. We also comment on (a) the generalization of our results to the case $P_M \neq 1$ and (b) the relation between D_m^\pm and the order- m moments of gradients of hydrodynamic fields, which are used in characterizing intermittency in turbulent flows.

PACS numbers: 47.27.Ak, 52.30.Cv, 47.27.ek, 02.30.Jr

Intermittency is widespread in nature: the characterization of such intermittency is a central problem in turbulence [1–9], in nonequilibrium statistical mechanics, in the production and storage of wind and solar energy, and the behaviors of market crashes and of several critical phenomena [10, 11]. Such intermittency has been studied extensively in fluid turbulence [1, 3–9] and in magnetohydrodynamic (MHD) turbulence [12–16], often by using order- p structure functions of fields such as the velocity and, in MHD, also the magnetic field. An example is the (longitudinal) velocity \mathbf{v} structure function $S_p(r) \equiv \langle [\delta v(r)]^p \rangle$, where $\delta v(r) \equiv [\mathbf{v}(\mathbf{x} + \mathbf{r}) - \mathbf{v}(\mathbf{x})] \cdot [\mathbf{r}/r]$, which scales as $S_p(r) \sim r^{\zeta_p}$, for $\eta_d \ll r \ll L$, where η_d is the dissipation length scale below which viscous dissipation is significant, L is the large length scale at which energy is injected into the fluid, and the multiscaling exponents ζ_p , which are nonlinear, monotone increasing functions of p , characterize the intermit-

tency [1]; simple scaling is obtained if ζ_p depends linearly on p as in the phenomenological approach (K41) of Kolmogorov [17].

The determination of ζ_p is a challenging task [5, 6, 9], which is especially more difficult for time-dependent structure functions [18, 19] or MHD turbulence [12–16]. Therefore, we explore other signatures of intermittency. For three-dimensional (3D) fluid turbulence Refs. [20–22] have introduced a new way of analyzing direct numerical simulations (DNSs) to obtain fresh insights into suitably scaled (see below), order- m moments D_m of the vorticity $\boldsymbol{\omega} = \nabla \times \mathbf{u}$. These studies show the following: (a) on theoretical grounds, three regimes, I, II, and III, are possible, with the D_m ordered in different ways (Fig. 1, Ref. [22]); but (b) *only regime I is observed in a wide variety of DNSs* [20–22]. Regime I has sufficiently depleted nonlinearity so that a global attractor exists, *if the solutions remain in region I*, as they do in all the DNSs examined so far from

this point of view.

We develop the analog of the above theoretical framework for the case of 3D MHD turbulence; then we examine the behaviors of D_m^\pm , the 3D MHD counterparts of D_m , in a variety of DNSs, which we have carried out independently in different groups, to obtain new insights into the depletion of nonlinearity here. We find that 3D MHD turbulence is like its fluid-turbulence counterpart inasmuch as all solutions remain in *only one regime, with depleted nonlinearity, in a large variety of DNSs*. We examine the implications of our results for the exponents q^\pm that characterize the power-law dependences of the energy spectra $\mathcal{E}^\pm(k)$ on the wave number k , in the inertial range of scales, ($2\pi/k$ much less than the energy-injection length scale and much greater than the length scale at which viscous and diffusive losses become significant).

The velocity \mathbf{u} and magnetic field \mathbf{b} can be combined into the Elsässer variables $\mathbf{z}^\pm = \mathbf{u} \pm \mathbf{b}$; with $\nu_\pm = [\nu \pm \eta]/2$, $\mathbf{f}^\pm = \mathbf{f}_u \pm \mathbf{f}_b$, the incompressible 3D MHD equations are

$$\partial_t \mathbf{z}^\pm + \mathbf{z}^\mp \cdot \nabla \mathbf{z}^\pm = -\nabla \mathcal{P} + \nu_+ \nabla^2 \mathbf{z}^\pm + \nu_- \nabla^2 \mathbf{z}^\mp + \mathbf{f}^\pm, \quad (1)$$

where $\nabla \cdot \mathbf{z}^\pm = 0$, \mathcal{P} is the total pressure, $\mathbf{j} = \nabla \times \mathbf{b}$ is the current density, and ν and η are, respectively, the kinematic viscosity and the magnetic diffusivity, whose ratio yields the magnetic Prandtl number $P_M = \nu/\eta$; and \mathbf{f}^\pm are the forcing terms, which are absent in decaying MHD turbulence. The Taylor-microscale Reynolds number $R_\Lambda = u_{rms} \sqrt{\langle \mathbf{u}^2 \rangle + \langle \mathbf{b}^2 \rangle} / (\nu \sqrt{\langle \boldsymbol{\omega}^2 \rangle + \langle \mathbf{j}^2 \rangle})$, with u_{rms} the root-mean-square velocity. Our DNSs of the 3D MHD equations use a periodic cubic box and a pseudospectral method [12–16] with large-scale initial conditions, and in some cases, forcing (Table I [23]).

For ideal 3D MHD (i.e., $\nu_\pm = 0$, $\mathbf{f}^\pm = 0$) the invariants are the energies $E_\pm = \frac{1}{2} \langle \mathbf{z}_\pm \cdot \mathbf{z}_\pm \rangle = E_T \pm H_C$ and the magnetic helicity $H_M = \langle \mathbf{A} \cdot \mathbf{b} \rangle$, where the vector potential \mathbf{A} yields $\mathbf{b} = \nabla \times \mathbf{A}$, $E_T = \frac{1}{2} \langle \mathbf{u} \cdot \mathbf{u} + \mathbf{b} \cdot \mathbf{b} \rangle = E_u + E_b$, and $H_C = \langle \mathbf{u} \cdot \mathbf{b} \rangle$. We define $\sigma_C = \cos(\mathbf{u}, \mathbf{b})$ and $\sigma_m = \cos(\mathbf{A}, \mathbf{b})$, the relative rates of cross and magnetic helicity, with $|\sigma_{c,m}| \leq 1$; they represent the degree to which the fields are aligned and they are measures, global or point-wise, of the strength of nonlinearities in MHD.

We obtain the evolution of the vorticity and the current, and thus of $\boldsymbol{\omega}^\pm = \boldsymbol{\omega} \pm \mathbf{j}$, by using standard vector identities [23]; for $P_M = 1$ we have

$$\begin{aligned} (\partial_t + \mathbf{z}^\mp \cdot \nabla) \boldsymbol{\omega}^\pm - \boldsymbol{\omega}^\mp \cdot \nabla \mathbf{z}^\pm - \nu \Delta \boldsymbol{\omega}^\pm - \nabla \times \mathbf{f}^\pm \\ = \boldsymbol{\omega}^\mp \times \boldsymbol{\omega}^\pm + \sum_{i=1}^3 \partial_i \mathbf{z}^\pm \times \partial_i \mathbf{z}^\mp. \end{aligned} \quad (2)$$

The two terms on the right-hand side stem from stem from the equation for the current; the labels $i = 1, 2$, and 3 refer respectively to x, y , and z [23].

The exact constraints because of conservation laws involve mixed (\mathbf{u}, \mathbf{b}) correlators [24, 25]. Dimensional analysis gives $\zeta_p^{IK} = p/4$, if we use the model of Iroshnikov and Kraichnan (IK) [26, 27] and assume $\sigma_C = 0$, or $\zeta_p^{K41} = p/3$, if we use K41 [16, 17]; and $\mathcal{E}^\pm(k) \sim k^{-3/2}$ (IK) or $\mathcal{E}^\pm(k) \sim k^{-5/3}$ (K41). Some models [28, 29] and DNS results [16, 30, 31] indicate that the departure from linear scaling, be it of the IK or K41 forms, is stronger in 3D MHD turbulence than it is in 3D Navier-Stokes (NS) turbulence, which suggests a depletion of nonlinearity by virtue of the tendency of alignment or anti-alignment of \mathbf{u} and \mathbf{b} .

We now describe our generalization of the analysis of Refs. [20–22], for the 3D NS equation, to the case of the 3D MHD equation [23]. We define the order- m scaled moments of $\boldsymbol{\omega}^\pm$:

$$\Omega_m^\pm(t) = \left(L^{-3} \int_V |\boldsymbol{\omega}^\pm|^{2m} dV \right)^{1/2m}; \quad (3)$$

$$D_m^\pm = (\varpi_0^{-1} \Omega_m^\pm)^{\alpha_m}, \quad \alpha_m = \frac{2m}{4m-3}; \quad (4)$$

here $\varpi_0 = \nu L^{-2}$ is the box-size frequency and the total volume $V = L^3$. A Hölder inequality implies that $\Omega_{m+1}^\pm(t) \geq \Omega_m^\pm(t) \geq \dots \geq \Omega_1^\pm(t)$; however, the D_m^\pm moments can scale with order m in different ways because α_m is a decreasing function of m . The choice of D_m , and the value of α_m [20], for the 3D NS equation, follow from the invariance of this equation under the transformations $\mathbf{x}' = a\mathbf{x}$, $t' = a^2 t$, $\mathbf{u}' = a^{-1}\mathbf{u}$, $\mathcal{P}' = a^{-2}\mathcal{P}$. For 3D MHD we must add $\mathbf{b}' = a^{-1}\mathbf{b}$; and we can then show that $\Omega_m^{\pm'} = [a^{-1/\alpha_m}] \Omega_m^\pm$ and define the coefficients $A_m^\pm(t) \equiv \ln D_m^{\pm'}(t) / \ln D_1^\pm(t)$.

We follow [21, 22] and introduce the Ansätze [32]

$$D_1^{\pm \frac{\sigma}{2}} \leq D_m^\pm \leq D_1^{\pm A_{m,\lambda}^\pm}, \quad A_{m,\lambda}^\pm = \frac{m\lambda^\pm + 1 - \lambda^\pm}{4m-3}, \quad (5)$$

where $A_{m,\lambda}^\pm$ is the maximum over time of $A_m^\pm(t)$ and $1 \leq \lambda_\pm \leq 4$, which implies that the nonlinearity is depleted here (cf. Eq.(1.4) and compare Eq.(3.7) and Eq.(3.12) in Ref.[22]). The lower bounds on λ^\pm follow from the Hölder inequality $\Omega_m^\pm \geq \Omega_1^\pm$; the upper bounds are treated as in the NS case [22].

We have more variables in the 3D-MHD case than in the 3D NS equation, so we introduce $X_1 \equiv D_1^+ + D_1^-$ and show [23]

$$\frac{\dot{X}_1^\pm}{2\varpi_0} \leq -\frac{X_1^2}{2E_0} + c_{6,m}X_1^{1+\frac{1}{2}\lambda^\pm - \frac{(\lambda^\pm - \lambda^\mp)}{4m}} + GrX_1^{1/2}, \quad (6)$$

where E_0 is a bounded and dimensionless measure of the energy, Gr the Grashof number, a dimensionless measure of the forcing term, and $c_{6,m}$ a constant. Hence, X_1 remains bounded if the negative term on the right-hand side of (6) dominates, which occurs if

$$1 + \frac{1}{2}\lambda^\pm - (\lambda^\pm - \lambda^\mp)/4m < 2, \quad (7)$$

or equivalently $\lambda^\pm < 2 + \epsilon_m^\pm$, where $\epsilon_m^\pm = (\lambda^\pm - \lambda^\mp)/2m$ is a small number [36]. Therefore, the *natural*, 3D-MHD analogs of Fig. 1 in Ref. [22] are the schematic plots of D_m^\pm versus D_1^+ and D_m^- versus D_1^- in Fig. 1, which show three regimes: For regular solutions, we must have $1 \leq \lambda^\pm \leq 2$ (regime I); when $2 \leq \lambda^\pm \leq 4$ (regime II), there is depletion, but not enough to control solutions; and, finally, at $\lambda_\pm = 4$ (regime III) we have $D_m^\pm \propto D_1^\pm$.

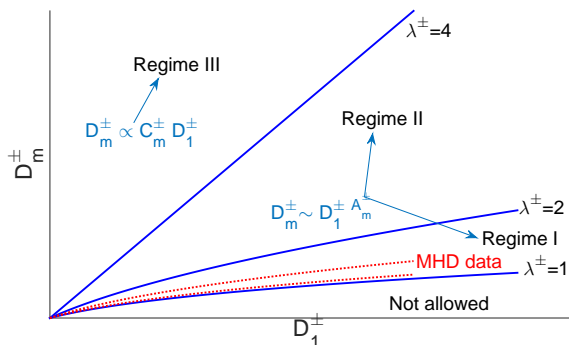


FIG. 1: (Color online) Schematic plots of D_m^+ versus D_1^+ and D_m^- versus D_1^- showing the three regimes I, II, and III for 3D MHD. Regularity can be proven if both D_1^+ and D_1^- lie in regimes I or III.

Our DNS data [23] indicate that regime I ($1 \leq \lambda^\pm \leq 2$) is obtained in 3D MHD for all the solu-

tions we study. In Fig. 2 we give representative results from four of our DNSs [23]. In the first column of Fig. 2, we give log-log (base 10) plots of the energy spectra $E(k)$ versus k ; the second column has plots of $A_m^+(t)$ versus t , from which we determine $A_{m,\lambda}^+$ (plots for $A_m^-(t)$ versus t are similar), which follow from $D_m^+(t)$.

Numerical trajectories do not follow exactly the schematic, concave curves of Figs. 1 (a) and (b), so we determine λ^\pm as follows (cf. Ref. [22] for the 3D-NS equation). We define λ_m^\pm to be those values that we compute from Eq. (5) for $A_{m,\lambda}^\pm$. In the third column of Fig. 2, we give plots of λ_m^\pm versus m , in the range $2 \leq m \leq 9$, for which we obtain good-quality numerical data. From these plots we obtain λ^\pm from the minimum over m of λ_m^\pm . In general, $1 \leq \lambda_\pm \leq 4$; however, in all our DNSs, $1 \leq \lambda_\pm \leq 2$, i.e., our solutions lie in regime I.

To examine the implications of our results for energy spectra, we define the dimensionless, time-averaged, inverse length scale $\kappa_{2,0} = \left[\frac{\|\nabla \omega^\pm\|_2}{\|z^\pm\|_2} \right]^{1/2}$ and obtain [23]

$$\langle L\kappa_{2,0}^\pm \rangle_T \leq c Re^{\frac{\lambda^\pm + 1}{4} + \frac{\lambda^\mp}{8}}, \quad (8)$$

where $Re = L\sqrt{2E_{\text{tot}}}/\nu$ is the *global* Reynolds number and $\langle \rangle_T$ stands for temporal average. If we assume isotropy and make the power-law Ansatz

$$\mathcal{E}^\pm(k) = \begin{cases} A k^{-q^\pm}, & L^{-1} \leq k \leq k_c^\pm, \\ 0, & k > k_c^\pm, \end{cases} \quad (9)$$

we obtain

$$\langle L\kappa_{2,0}^\pm \rangle_T \sim (Lk_c^\pm)^{1 - \frac{q^\pm - 1}{4}} \sim Re^{\frac{5 - q^\pm}{4(3 - q^\pm)}}, \quad (10)$$

(see Eqs.(??-??) in [23]). We thus get

$$q^\pm \geq 3 - \frac{4}{2\lambda^\pm + \lambda^\mp} \geq \frac{5}{3}, \quad (11)$$

which excludes the IK exponent $3/2$, at least in the absence of intermittency. However, we have assumed full isotropy at all scales and the limit $Re \rightarrow \infty$ when comparing (8) and (10). Furthermore, (10) implicitly assumes $E_+ = E_-$. In the general [23], this relation is modified leading to a set of inequalities for the q^\pm that do not exclude IK.

In Fig. 3 we display plots of $\langle D_m^+ \rangle$ versus R_Λ , where the angular brackets now indicate the average over the statistically stationary turbulent

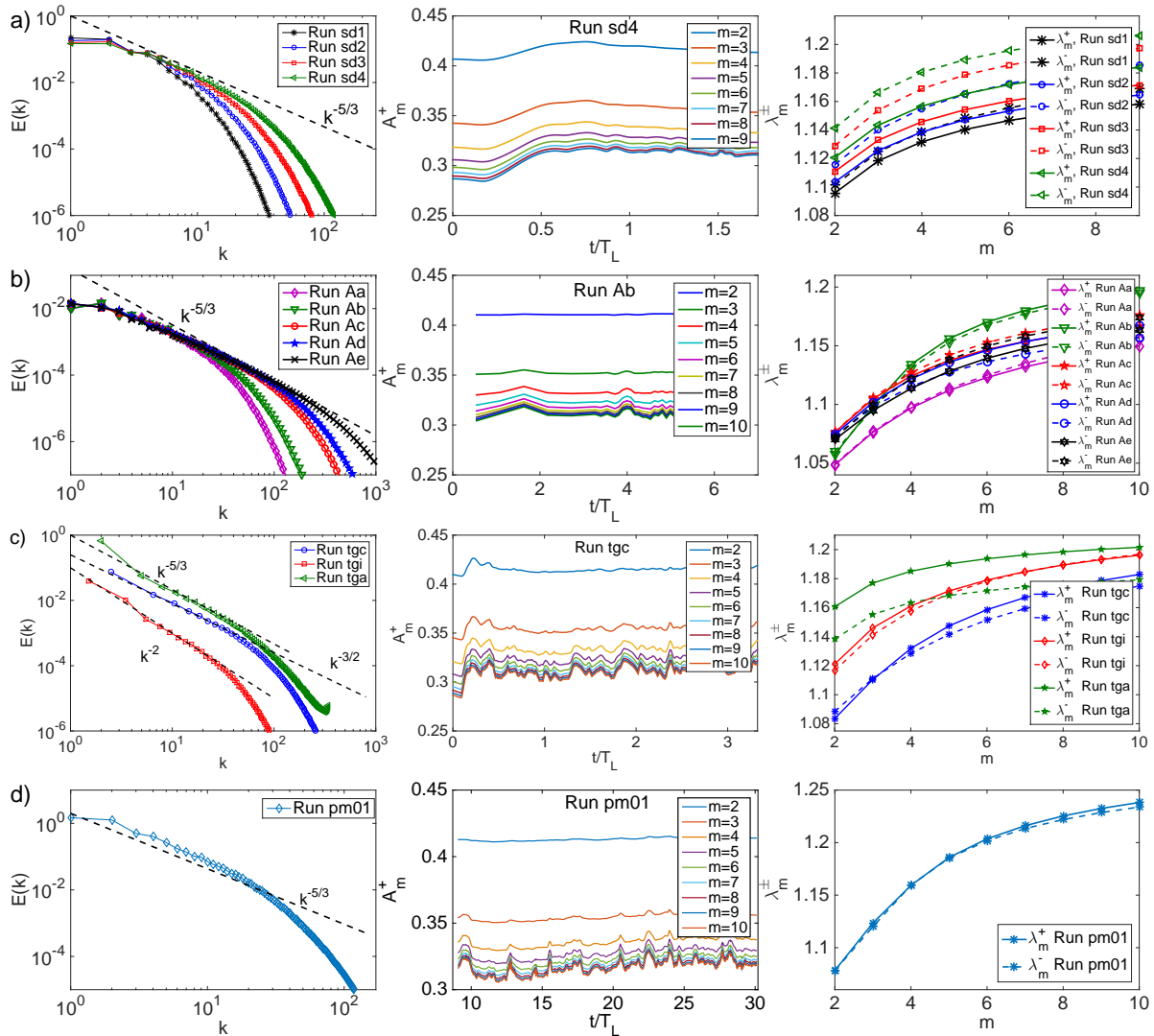


FIG. 2: (Color online) Representative results from our DNSs: total energy spectra (first column), temporal evolution of A_m^\pm (second column) and values of λ_m^\pm (third column). The rows correspond to different runs: a) decaying 3D MHD turbulence, b) forced, statistically steady 3D MHD turbulence, c) forced, statistically steady 3D MHD turbulence with imposed Taylor-Green symmetries and d) forced, statistically steady 3D MHD turbulence with $P_M = 0.1$. For parameters see Table I in [23]

state; we present data (pentagrams in Fig. 3) from the runs Aa-Ae (Table I in [23]). Circles indicate decaying-MHD data points (runs sd1-sd4); here we use the value of D_m^+ at the time at which the energy-dissipation rate ϵ reaches its first maximum [16]. The order- m moments of gradients, or *gradmoments*, of hydrodynamic fields have been used to investigate Nelkin scaling [33–35], i.e., the power-law dependence of the gradmoments on the Reynolds number Re in the case of fluid turbulence; the Nelkin-scaling exponents ξ_m can be related to the structure-function exponents ζ_m [33–

35]. Our vorticity moments are upper bounds for gradmoments of the Elsässer variables by virtue of the Riesz transform (see Eq. (1.11) in [23]). If these bounds are saturated, then the exponents, which we extract from the plots of Fig. 3, should be related to the Nelkin exponents for 3D MHD turbulence. We defer a detailed exposition of such scaling in 3D MHD to another study.

In liquid metals, as well as in the solar photosphere, P_M is very small. It can also be very large as, e.g., in the interstellar medium. Our mathematical analysis in [23] is not valid if $P_M \neq 1$ be-

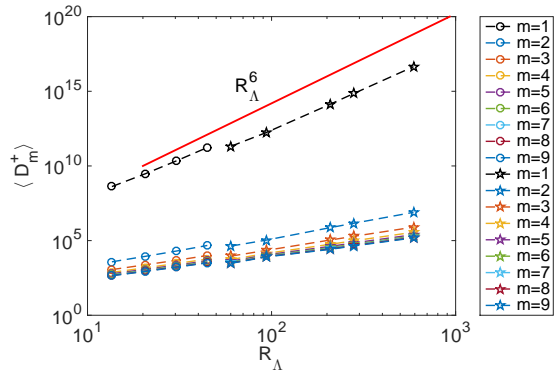


FIG. 3: (Color online) Plots versus R_Λ of $\langle D_m^+ \rangle$, for the runs Aa-Ae (pentagrams) and its decaying-MHD analog, for the runs sd1-sd4 (circles), where we use the value of D_m^+ at the time at which the energy dissipation rate ϵ reaches its first maximum [16]. See Table I in [23] for additional information about these runs.

cause ν_- can become negative for $P_M \leq 1$. However, our DNS results in Fig. 3 show that plots for $P_M = 0.1$ (bottom row) are similar to their counterparts for $P_M = 1$ (top three rows). Furthermore, we see from Table I (Supplemental Material [23]), at least for a fixed value of ν , that the values of λ_m^\pm are comparable to their $P_M = 1$ counterparts; these values of λ^\pm decrease marginally as we increase P_M .

Our work, which builds upon the studies of Refs. [20–22] for fluid turbulence, provides new insights into the depletion of nonlinearity in 3D MHD turbulence and its intermittency. In particular, we introduce the scaled moments D_m^\pm , and then obtain inequalities containing D_m^\pm and D_1^\pm ; these inequalities specify three possible regimes. We find that 3D MHD turbulence is like its fluid-turbulence counterpart insofar as all solutions, which we have investigated, remain in only one regime; this regime I (Fig. 1) displays depleted nonlinearity. Our results lead to the inequality (11) for the spectral exponents q^\pm , if we make the assumption of isotropy. We suggest that the Riesz transform can relate D_m^\pm and the order- m moments of gradients of the hydrodynamic fields; such moments can then be used, along with a suitable generalization of Nelkin scaling [33–35] for 3D MHD turbulence, to relate slopes of plots like those in Fig. 3 to the multiscaling exponents of Elsässer-field structure functions. We conclude that 3D MHD appears to have more nonlinear

depletion than does fluid turbulence, because the values of λ^\pm are lower than those for their fluid-turbulence counterparts; this can be attributed to Alfvén waves weakening the nonlinear eddies.

Acknowledgments: We thank H. Homann and R. Grauer for providing the data of runs Ad and Ae. Data from runs Ad and Ae of H. Homann and R. Grauer was produced on the IBM BlueGene/P computer JUGENE at the FZ Juelich that was available through the “XXL project of HBO28”. We also acknowledge U. Frisch and D. Vincenzi for useful discussions. The computations for runs sd1-sd4 were performed on Janus (CU Boulder). Runs Aa-Ac and tg were performed at Mésocentre SIGAMM hosted at the Observatoire de la Côte d’Azur and CICADA hosted by the University of Nice-Sophia. Computer time was also provided by GENCI on the IDRIS/CINES/TGCC clusters. JG and AP thank Fédération Doebelin for support. RP thanks the Department of Science and Technology (India) for support and SERC (IISc) for computational resources. AG is grateful for support through a grant from the European Research Council (ERC) under the European Community’s Seventh Framework Programme (FP7/2007-2013)/ERC Grant Agreement No. 297004. GS acknowledges support from the ERC Advanced Grant “NewTURB”, No. 339032. GK thanks the Indo-French Centre for Applied Mathematics (IFCAM) for supporting a visit during which parts of this paper were written. JS is supported by the National Science Foundation (NSF) Graduate Research Fellowship Program (GRFP) under Grant No. DGE 1144083.

-
- [1] U. Frisch, *Turbulence: The Legacy of A. N. Kolmogorov* (Cambridge University Press, Cambridge, 1995).
 - [2] R. Kerr, *J. Fluid Mech.* **153**, 31 (1985).
 - [3] C. Meneveau and K. R. Sreenivasan, *J. Fluid Mech.* **224**, 429 (1991).
 - [4] K. R. Sreenivasan and R. A. Antonia, *Ann. Rev. Fluids Mech.* **29**, 435 (1997).
 - [5] G. Boffetta, A. Mazzino, and A. Vulpiani, *J. Phys. A: Mathematical and Theoretical* **41**, 363001 (2008).
 - [6] A. Arneodo, R. Benzi, J. Berg, L. Biferale, E. Bodenschatz, A. Busse, E. Calzavarini, B. Castaing, M. Cencini, L. Chevillard, et al., *Phys. Rev. Lett.*

- 100**, 254504 (2008).
- [7] D. Donzis, P. Yeung, and K. Sreenivasan, *Phys. Fluids* **20**, 045108 (2008).
- [8] T. Ishihara, T. Gotoh, and Y. Kaneda, *Annu. Rev. Fluid Mech.* **41**, 16 (2009).
- [9] R. Pandit, P. Perlekar, and S. S. Ray, *Pramana, Journal of Physics* **73**, 157 (2009).
- [10] S. Bramwell, P. Holdsworth, and J. Pinton, *Nature* **396**, 552 (1998).
- [11] D. Sornette, Springer-Verlag Berlin Heidelberg (2006).
- [12] D. Biskamp and W.-C. Muller, *Phys. Plasmas* **7**, 4889 (2000).
- [13] W.-C. Muller and D. Biskamp, *Phys. Rev. Lett.* **84**, 475 (2000).
- [14] P. D. Mininni and A. Pouquet, *Phys. Rev. Lett.* **99**, 254502 (2007).
- [15] P. D. Mininni and A. Pouquet, *Phys. Rev. E* **80**, 025401 (2009).
- [16] G. Sahoo, P. Perlekar, and R. Pandit, *New J. Physics* **13**, 013036 (2011).
- [17] A. N. Kolmogorov, *Dokl. Akad. Nauk SSSR* **32**, 16 (1941).
- [18] D. Mitra and R. Pandit, *Phys. Rev. Lett.* **93**, 024501 (2004).
- [19] S. S. Ray, D. Mitra, and R. Pandit, *New J. Phys.* **10**, 033003 (2008).
- [20] J. Gibbon, *J. Math. Phys.* **53**, 115608 (2012).
- [21] D. Donzis, J. Gibbon, A. Gupta, R. Kerr, R. Pandit, and D. Vincenzi, *J. Fluid Mech.* **732**, 316 (2013).
- [22] J. Gibbon, D. Donzis, A. Gupta, R. Kerr, R. Pandit, and D. Vincenzi, *Nonlinearity* **27**, 2605 (2014).
- [23] Supplementary material (2015).
- [24] H. Politano, T. Gomez, and A. Pouquet, *Phys. Rev. E* **68**, 026315 (2003).
- [25] A. Basu, A. Naji, and R. Pandit, *Phys. Rev. E* **89**, 012117 (2014).
- [26] P. S. Iroshnikov, *Sov. Astron.* **7**, 566 (1963).
- [27] R. H. Kraichnan, *Phys. Fluids* **8**, 1385 (1965).
- [28] R. Grauer, J. Krug, and C. Mariani, *Phys. Lett. A* **195**, 335 (1994).
- [29] H. Politano and A. Pouquet, *Phys. Rev. E* **52**, 636 (1995).
- [30] H. Politano, V. Carbone, and A. Pouquet, *Europhys. Lett.* **43**, 516 (1998).
- [31] W. C. Müller, D. Biskamp, and R. Grappin, *Phys. Rev. E* **67**, 066302 (2003).
- [32] J. D. Gibbon, ArXiv:1506.03060v2 (2015).
- [33] M. Nelkin, *Phys. Rev. A* **42**, 7226 (1990).
- [34] J. Schumacher, K. R. Sreenivasan, and V. Yakhot, *New J. Phys.* **9**, 89 (2007).
- [35] S. Chakraborty, U. Frisch, W. Pauls, and S. S. Ray, *Phys. Rev. E* **85**, 015301(R) (2012).
- [36] Standard analysis leads to a term $\propto X_1^3$ in Eq.(6) (see Ref. [22] for the NS case), which does not lead to a control over the solutions at large times.

Supplemental Material for Depletion of Nonlinearity in Magnetohydrodynamic Turbulence: Insights from Analysis and Simulations

J. Gibbon¹, A. Gupta², G. Krstulovic³, R. Pandit⁴, H.

Politano⁵, Y. Ponty³, A. Pouquet^{6,7}, G. Sahoo², and J. Stawarz⁷

¹*Department of Mathematics, Imperial College London, London SW7 2AZ, UK.*

²*Department of Physics, University of Rome 'Tor Vergata', 00133 Roma, Italy.*

³*Laboratoire Lagrange, Université Côte d'Azur, Observatoire de la Côte d'Azur,*

CNRS, Blvd de l'Observatoire, CS 34229, 06304 Nice cedex 4, France

⁴*Centre for Condensed Matter Theory, Indian Institute of Science, Bangalore, 560 012, India.*

⁵*Laboratoire Dieudonné, Université de Nice, France.*

⁶*National Center for Atmospheric Research,*

P.O. Box 3000, Boulder, CO 80307, USA.

⁷*Laboratory for Atmospheric and Space Physics,*

University of Colorado, Boulder, CO 80309, USA.

PACS numbers: 47.27.i, 47.65.d, 47.27.Ak, 02.30.Jr

In this Supplemental Material we give some technical details leading to the results presented in the Letter. Part I contains a Table of the runs described in this paper. Part II contains the mathematical analysis used in this Letter. In particular, in Part II A we give the mathematical steps required to obtain an estimate of the temporal evolution of the vorticity moment D_1^\pm , and in II B the steps leading to the spectrum. In Part III the Doering-Foias Grashof-Reynolds relation is obtained for MHD. Part IV deals with an estimate of the cut-off wave numbers, both for fluids and MHD; and finally Part V contains the derivation of the equation for the current and the ω^\pm vorticities.

I. TABLE OF RUNS

In Table I we give the parameters for the runs analyzed in this paper. All runs are performed in three dimensions by using periodic boundary conditions, no imposed external magnetic field and a magnetic Prandtl number P_M of unity, except for the pm runs; no modeling of the small scales is employed. For the sd runs, which are spin-down, the Reynolds number is varied. Initial condition for the spin-down runs sd is the three-dimensional Orszag-Tang vortex [1], with added phase shifts to set $\sigma_C \simeq -0.21$ initially. The Aa-Ae runs are high-resolution forced runs [2, 3], with a constant velocity and magnetic forcing for which all the modes in the first two Fourier shells are kept constant. From Aa to Ae runs, the resolution increases with the Reynolds number. The tg runs are forced in both the velocity and induction equations; in these runs, the four-fold symmetries of the Taylor-Green vortex extended to MHD are implemented. Moreover, the three runs have different resulting energy spectra (IK, K41, and k^{-2}), although they have the same ideal invariants [4]. Finally, the pm runs have a fixed viscosity, but variable magnetic diffusivities and thus allow for extending the analysis to the case of $P_M \neq 1$ (see [5]).

II. MATHEMATICAL ANALYSIS

A. Control of the D_1^\pm -variables under depletion for the 3D MHD-Elsässer system

The relevant PDEs in Elsässer variables are ($\mathbf{z}^\pm = \mathbf{u} \pm \mathbf{B}$)

$$(\partial_t + \mathbf{z}^\mp \cdot \nabla) \mathbf{z}^\pm = \nu \Delta \mathbf{z}^\pm - \nabla P^\pm + \mathbf{f}^\pm(\mathbf{x}), \quad (\text{II.1})$$

TABLE I: Parameters for our direct numerical simulations. $k_{\max} = N/3$ is the maximum resolved wavenumber at grid resolution N (the standard 2/3 de-aliasing rule). $\Lambda_T = \sqrt{\langle \mathbf{u}^2 \rangle + \langle \mathbf{b}^2 \rangle} / \sqrt{\langle \boldsymbol{\omega}^2 \rangle + \langle \mathbf{j}^2 \rangle}$ is the Taylor scale based on the total energy $E_T = E_V + E_M$, and $R_\Lambda = u_{rms} \Lambda_T / \nu$ is the Taylor Reynolds number based on that scale ($u_{rms} = \sqrt{2E_V/3}$). σ_C and σ_M are the relative rates of cross-helicity and magnetic helicity, respectively. λ^\pm are the parameters extracted from the data for high m (subscript max) and low m (subscript min) (See Fig.??, column 3 in the Letter).

Run	N	R_Λ	Λ_T	P_M	σ_C	σ_M	λ_{\min}^+	λ_{\max}^+	λ_{\min}^-	λ_{\max}^-
sd1	128	14	0.27	1	-0.27	-0.22	1.096	1.158	1.101	1.169
sd2	256	21	0.20	1	-0.27	-0.23	1.103	1.165	1.116	1.186
sd3	512	30	0.15	1	-0.27	-0.24	1.111	1.171	1.129	1.197
sd4	768	45	0.11	1	-0.26	-0.24	1.121	1.184	1.141	1.206
Aa	512	35	0.098	1	0.019	0.003	1.049	1.150	1.049	1.156
Ab	1024	54	0.074	1	0.017	0.004	1.057	1.197	1.060	1.195
Ac	2048	120	0.036	1	0.011	Data Not Available	1.076	1.167	1.076	1.176
Ad	2048	161	0.027	1	0.009	Data Not Available	1.074	1.168	1.073	1.157
Ae	4096	341	0.014	1	0.010	Data Not Available	1.070	1.163	1.072	1.174
tgi	1024	100	0.066	1	0	0	1.121	1.196	1.117	1.197
tga	1024	83	0.084	1	0	0	1.161	1.202	1.138	1.202
tgc	1024	110	0.056	1	~ 0.05	0	1.084	1.183	1.089	1.175
pm01	512	240	0.14	0.1	0.122	0.0047	1.078	1.238	1.078	1.234
pm02	512	140	0.10	1.0	0.075	0.0049	1.070	1.171	1.069	1.160
pm03	512	80	0.06	10	0.226	0.0077	1.053	1.149	1.052	1.158

together with $\text{div } \mathbf{z}^\pm = 0$. With $\boldsymbol{\omega}^\pm$ defined as $\boldsymbol{\omega}^\pm = \text{curl } \mathbf{z}^\pm$, we have

$$(\partial_t + \mathbf{z}^\mp \cdot \nabla) \boldsymbol{\omega}^\pm = \nu \Delta \boldsymbol{\omega}^\pm + \boldsymbol{\omega}^\mp \cdot \nabla \mathbf{z}^\pm + \boldsymbol{\omega}^\mp \times \boldsymbol{\omega}^\pm + \sum_{i=1}^3 \partial_i \mathbf{z}^\pm \times \partial_i \mathbf{z}^\mp + \text{curl } \mathbf{f}^\pm. \quad (\text{II.2})$$

The label $i = 1, 2, 3$ in the fourth term on the right hand side refers to the derivatives x, y and z . To proceed, it is necessary to define the respective Reynolds and Grashof numbers. Two ‘‘velocities’’, U^\pm , based on the squared, time-averaged L^2 -norms of \mathbf{z}^\pm ($\|\cdot\|_2$), are defined as

$$U^{\pm 2} = L^{-3} \langle \|\mathbf{z}^\pm\|_2^2 \rangle_T, \quad (\text{II.3})$$

where $\langle \cdot \rangle_T$ means the time-average up to a long time T . In turn, the U^\pm define two Reynolds numbers

$$Re_\pm = LU^\pm / \nu. \quad (\text{II.4})$$

The Reynolds numbers are based on average velocities, two Grashof numbers Gr_\pm are based on the forcing functions \mathbf{f}^\pm , namely,

$$Gr_\pm = L^{3/2} \|\mathbf{f}^\pm\|_2 / \nu^2. \quad (\text{II.5})$$

For the class of forcing functions that is concentrated around a single length-scale ($\ell = L$ for the purposes of this paper), a relation exists between Gr_\pm and Re_\pm for solutions of (II.1). This has been derived through the method of Doering-Foias [6] (see Part II.33) where it has been deduced that for large Gr_\pm ,

$$Gr_\pm \leq c Re_\pm (Re_\mp + 1). \quad (\text{II.6})$$

The constant c depends on the shape of the forcing [6].

To proceed, we first use the definition

$$\Omega_m^\pm(t) = \left(L^{-3} \int_{\mathcal{V}} |\omega^\pm|^{2m} dV \right)^{1/2m}. \quad (\text{II.7})$$

Each of the Ω_m^\pm are standard L^{2m} -norms scaled with the system volume so they have the dimension of a frequency. Then we use the following scaling that was introduced in work on the 3D Navier-Stokes equations [7, 8] through (invariance) scaling arguments [9]

$$D_m^\pm = (\varpi_0^{-1} \Omega_m^\pm)^{\alpha_m}, \quad \alpha_m = \frac{2m}{4m-3}, \quad (\text{II.8})$$

where $\varpi_0 = \nu L^{-2}$ is the box frequency. Now we proceed under the assumption that (II.1) has a solution and look at the evolution of D_1^\pm :

$$\begin{aligned} \frac{1}{2} \varpi_0^{-1} \dot{D}_1^\pm &\leq -L^{-1} \varpi_0^{-2} \int_{\mathcal{V}} |\nabla \omega^\pm|^2 dV + L^{-3} \varpi_0^{-3} \int_{\mathcal{V}} |\omega^\pm \cdot (\omega^\mp \cdot \nabla z^\pm)| dV \\ &+ L^{-3} \varpi_0^{-3} \sum_{i=1}^3 \int_{\mathcal{V}} |\omega^\pm \cdot (\partial_i z^\pm \times \partial_i z^\mp)| dV + Gr_\pm D_1^{\pm 1/2}. \end{aligned} \quad (\text{II.9})$$

To estimate the first nonlinear term in (II.9) we write ($1 < m < \infty$)

$$\begin{aligned} \int_{\mathcal{V}} |\omega^\pm \cdot (\omega^\mp \cdot \nabla z^\pm)| dV &\leq \int_{\mathcal{V}} |\omega^\pm|^{\frac{2m-3}{2(m-1)}} |\omega^\pm|^{\frac{1}{2(m-1)}} |\omega^\mp|^{\frac{2m-3}{2(m-1)}} |\omega^\mp|^{\frac{1}{2(m-1)}} |\nabla z^\pm| dV \\ &\leq c_{1,m} \left(\int_{\mathcal{V}} |\omega^\pm|^2 dV \right)^{\frac{2m-3}{4(m-1)}} \left(\int_{\mathcal{V}} |\omega^\pm|^{2m} dV \right)^{\frac{1}{4m(m-1)}} \\ &\times \left(\int_{\mathcal{V}} |\omega^\mp|^2 dV \right)^{\frac{2m-3}{4(m-1)}} \left(\int_{\mathcal{V}} |\omega^\mp|^{2m} dV \right)^{\frac{1}{4m(m-1)}} \left(\int_{\mathcal{V}} |\omega^\pm|^{2m} dV \right)^{1/2m}. \end{aligned} \quad (\text{II.10})$$

Note that the sum of the five exponents in the latter expression is unity. For the last term we have invoked the inequality [14], which requires a Riesz transform in its proof, namely ,

$$\|\nabla z^\pm\|_{2m} \leq c_{2,m} \|\omega\|_{2m}, \quad (\text{II.11})$$

provided $1 \leq m < \infty$. Then (II.10) becomes

$$\begin{aligned} L^{-3} \varpi_0^{-3} \int_{\mathcal{V}} |\omega^\pm \cdot (\omega^\mp \cdot \nabla z^\pm)| dV &\leq c_{3,m} [D_1^\pm]^{\frac{2m-3}{4(m-1)}} [D_m^\pm]^{\frac{1}{2\alpha_m(m-1)}} \\ &\times [D_1^\mp]^{\frac{2m-3}{4(m-1)}} [D_m^\mp]^{\frac{1}{2\alpha_m(m-1)}} [D_m^\pm]^{\frac{1}{\alpha_m}}. \\ &\leq c_{3,m} [D_1^\pm]^{\frac{2m-3}{4(m-1)}} [D_m^\pm]^{\frac{2m-1}{2\alpha_m(m-1)}} \\ &\times [D_1^\mp]^{\frac{2m-3}{4(m-1)}} [D_1^\mp]^{\frac{1}{2\alpha_m(m-1)}}. \end{aligned} \quad (\text{II.12})$$

Now we insert the numerically observed depletion [15] discussed in the Letter (see also [8] for the NS case):

$$D_m^\pm \leq D_1^{A_{m,\lambda}^\pm} \quad \text{with} \quad \chi_m^\pm = A_{m,\lambda}^\pm (4m-3), \quad (\text{II.13})$$

where, for $2 \leq m \leq 9$, $A_{m,\lambda}$ is defined as

$$A_{m,\lambda}^\pm = \frac{m\lambda^\pm + 1 - \lambda^\pm}{4m-3}, \quad (\text{II.14})$$

and where the range of values of λ^\pm has been determined numerically (see main text of the Letter and Table I). By using this in (II.12) we find

$$L^{-3} \varpi_0^{-3} \int_{\mathcal{V}} |\omega^\pm \cdot (\omega^\mp \cdot \nabla z^\pm)| dV \leq c_{4,m} [D_1^\pm]^{\frac{\chi_m^\pm (2m-1) + m(2m-3)}{4m(m-1)}} [D_1^\mp]^{\frac{\chi_m^\mp + m(2m-3)}{4m(m-1)}}. \quad (\text{II.15})$$

Next we consider the second nonlinear term in (II.9) and use (II.11). From this, we find that the estimate for the right hand side of (II.15) is the same as in (II.10), apart from the constant $c_{5,m}$:

$$\begin{aligned} \sum_{i=1}^3 \int_{\mathcal{V}} |\boldsymbol{\omega}^{\pm} \cdot (\partial_i \mathbf{z}^{\pm} \times \partial_i \mathbf{z}^{\mp})| dV &\leq c_{5,m} \left(\int_{\mathcal{V}} |\boldsymbol{\omega}^{\pm}|^2 \right)^{\frac{2m-3}{4(m-1)}} \left(\int_{\mathcal{V}} |\boldsymbol{\omega}^{\pm}|^{2m} \right)^{\frac{1}{4m(m-1)}} \\ &\times \left(\int_{\mathcal{V}} |\boldsymbol{\omega}^{\mp}|^2 \right)^{\frac{2m-3}{4(m-1)}} \left(\int_{\mathcal{V}} |\boldsymbol{\omega}^{\mp}|^{2m} \right)^{\frac{1}{4m(m-1)}} \left(\int_{\mathcal{V}} |\boldsymbol{\omega}^{\pm}|^{2m} \right)^{1/2m}, \end{aligned}$$

so, converting this into the D_m^{\pm} , gives the same right hand side as in (II.15) but with a different constant $c_{2,m}$.

Taking all these terms together, and adding the two constants $c_{1,m}$ and $c_{2,m}$ to make the new constant $c_{3,m}$, (II.9) becomes

$$\frac{1}{2} \varpi_0^{-1} \dot{D}_1^{\pm} \leq -L^{-1} \varpi_0^{-2} \int_{\mathcal{V}} |\nabla \boldsymbol{\omega}^{\pm}|^2 dV + c_{6,m} [D_1^{\pm}]^{\frac{\chi_m^{\pm}(2m-1)+m(2m-3)}{4m(m-1)}} [D_1^{\mp}]^{\frac{\chi_m^{\mp}+m(2m-3)}{4m(m-1)}} + Gr_{\pm} D_1^{\pm 1/2}. \quad (\text{II.16})$$

To handle the coupled nature of the \pm -variables we define

$$X_1 = D_1^{\pm} + D_1^{\mp} \quad \text{and} \quad E_0 = \max_t (E^+, E^-) \quad (\text{II.17})$$

and the two bounded dimensionless energies are defined by $E^{\pm} = \nu^{-2} L^{-1} \int_{\mathcal{V}} |\mathbf{z}^{\pm}|^2 dV$. By adding the \pm -equations and using the depletion formulae (II.13) and (II.14), we obtain

$$\frac{1}{2} \varpi_0^{-1} \dot{X}_1 \leq -\frac{X_1^2}{2E_0} + c_{6,m} X_1^{1+\frac{1}{2}\lambda^{\pm} - (\lambda^{\pm} - \lambda^{\mp})/4m} + 2 \max(Gr_+, Gr_-) X_1^{1/2}. \quad (\text{II.18})$$

Because E_0 is bounded above, we have an absorbing ball for X_1 provided that

$$1 + \frac{1}{2}\lambda^{\pm} - (\lambda^{\pm} - \lambda^{\mp})/4m < 2. \quad (\text{II.19})$$

By this we mean that there is a ball of finite radius (depending on the upper bound on E_0) into which solutions are drawn if initial conditions are set outside the ball, and which cannot escape if initial conditions are set inside. (II.19) means that λ^{\pm} must satisfy

$$\lambda^{\pm} < 2 + \epsilon_m^{\pm}, \quad (\text{II.20})$$

where $\epsilon_m^{\pm} = (\lambda^{\pm} - \lambda^{\mp})/2m$, which is small.

B. Estimating the spectrum for the 3D MHD-Elsässer system

At this point we follow the method of Doering and Gibbon [10] which explains how to estimate average length scales and a corresponding equivalent spectrum by using some ideas in [11].

Step 1: We need to define a set of time-averaged inverse length scales[16]

$$\langle L^2 \kappa_{2,1}^{\pm 2} \rangle_T = \left\langle \frac{L^2 \|\nabla \boldsymbol{\omega}^{\pm}\|_2^2 dV}{\|\boldsymbol{\omega}^{\pm}\|_2^2} \right\rangle_T = \left\langle \frac{L^{-1} \varpi_0^{-2} \int_{\mathcal{V}} |\nabla \boldsymbol{\omega}^{\pm}|^2 dV}{D_1^{\pm}} \right\rangle_T, \quad (\text{II.21})$$

where the labelling of the subscripts is based on the number of derivatives on \mathbf{z}^{\pm} . Dividing (II.16) by D_1^{\pm} and time averaging, we find[17]

$$\begin{aligned} \langle L^2 \kappa_{2,1}^{\pm 2} \rangle_T &\leq c_{6,m} \left\langle [D_1^{\pm}]^{\frac{(\chi_m^{\pm} - m)(2m-1)}{4m(m-1)}} [D_1^{\mp}]^{\frac{\chi_m^{\mp} + m(2m-3)}{4m(m-1)}} \right\rangle_T \\ &\leq c_{6,m} \langle D_1^{\pm} \rangle_T^{\frac{(\chi_m^{\pm} - m)(2m-1)}{4m(m-1)}} \langle D_1^{\mp} \rangle_T^{\frac{\chi_m^{\mp} + m(2m-3)}{4m(m-1)}}. \end{aligned} \quad (\text{II.22})$$

Step 2: To estimate $\langle D_1^\pm \rangle_T$ we use the energy inequality version of (II.1)

$$\frac{1}{2} \frac{d}{dt} \|\mathbf{z}^\pm\|_2^2 \leq -\nu \|\boldsymbol{\omega}^\pm\|_2^2 + \|\mathbf{z}^\pm\|_2 \|\mathbf{f}^\pm\|_2, \quad (\text{II.23})$$

so by time averaging, converting into a dimensionless form, and using (II.6), we find that

$$\langle D_1^\pm \rangle_T \leq Gr_\pm Re_\pm \leq c Re_\pm^2 (Re_\mp + 1). \quad (\text{II.24})$$

Moreover, if we also define

$$\kappa_{1,0}^{\pm 2} = \frac{\|\boldsymbol{\omega}^\pm\|_2^2}{\|\mathbf{z}^\pm\|_2^2}, \quad \kappa_{2,0}^{\pm 4} = \frac{\|\nabla \boldsymbol{\omega}^\pm\|_2^2}{\|\mathbf{z}^\pm\|_2^2}, \quad (\text{II.25})$$

then, adapting ideas in [10], (II.23) gives

$$\langle L^2 \kappa_{1,0}^{\pm 2} \rangle_T \leq Re_\pm. \quad (\text{II.26})$$

Then it is easily shown that

$$\langle L \kappa_{2,0}^\pm \rangle_T \leq \langle L^2 \kappa_{2,1}^{\pm 2} \rangle_T^{1/4} \langle L^2 \kappa_{1,0}^{\pm 2} \rangle_T^{1/4}; \quad (\text{II.27})$$

and so from (II.21), (II.26) and (II.24), in which we keep only the dominant term, we find that

$$\begin{aligned} \langle L \kappa_{2,0}^\pm \rangle_T &\leq c_{6,m} [Re_\pm^2 (Re_\mp + 1)]^{\frac{(\chi_m^\pm - m)(2m-1) + \chi_m^\mp + m(2m-3)}{16m(m-1)}} Re_\pm^{1/4} \\ &\leq c_{6,m} Re_\pm^{\frac{(2m-1)\chi_m^\pm + \chi_m^\mp + 2m(m-2)}{8m(m-1)}} (Re_\mp + 1)^{\frac{\chi_m^\pm (2m-1) + \chi_m^\mp - 2m}{16m(m-1)}} \\ &\equiv c_{6,m} Re_\pm^{\sigma_m^\pm} (Re_\mp + 1)^{\rho_m^\mp}, \end{aligned} \quad (\text{II.28})$$

where, with $\chi_m^\pm = (m-1)\lambda^\pm + 1$,

$$\sigma_m^\pm = \frac{\lambda^\pm + 1}{4} + \left(\frac{\lambda^\mp - \lambda^\pm}{8m} \right), \quad \rho_m^\mp = \frac{(2m-1)\lambda^\mp + \lambda^\pm}{16m}. \quad (\text{II.29})$$

Thus, we can write (II.29) as

$$\langle L \kappa_{2,0}^\pm \rangle_T \leq c Re_\pm^{\frac{\lambda^\pm + 1}{4}} Re_\mp^{\frac{\lambda^\mp}{8}}; \quad (\text{II.30})$$

where we have ignored the factor of unity in the large Re^\pm -limit and taken the limit of large m . Then the problem is whether it is possible to consider Re_+ and Re_- as independent variables or not. The simplest way is to note that

$$\|\mathbf{z}^\pm\|^2 \leq \|\mathbf{v}\|^2 + 2\|\mathbf{v}\|\|\mathbf{b}\| + \|\mathbf{b}\|^2 \leq 2(\|\mathbf{v}\|^2 + \|\mathbf{b}\|^2) = 4E_{\text{tot}}. \quad (\text{II.31})$$

Defining a *global* Reynolds number as $Re = L\sqrt{2E_{\text{tot}}}/\nu$ (II.30) gives

$$\langle L \kappa_{2,0}^\pm \rangle \leq c Re^{\frac{\lambda^\pm + 1}{4} + \frac{\lambda^\mp}{8}}. \quad (\text{II.32})$$

Step 3: To interpret (II.32) in terms of statistical turbulence theory (restricting attention to forcing at the longest wavelength $\ell = L$), we follow the standard arguments in [11]. Suppose that Gr_\pm is high enough and the resulting flow is turbulent, ergodic, and isotropic enough in the limit $T \rightarrow \infty$, such that the wave-numbers $\langle \kappa_{n,0}^\pm \rangle_T$ may be identified with the moments of the energy spectrum $\mathcal{E}^\pm(k)$ according to

$$\lim_{T \rightarrow \infty} \langle \kappa_{n,0}^\pm \rangle_T := \left(\frac{\int_{L^{-1}}^{\infty} k^{2n} \mathcal{E}^\pm(k) dk}{\int_{L^{-1}}^{\infty} \mathcal{E}^\pm(k) dk} \right)^{1/2n}. \quad (\text{II.33})$$

The *a priori* constraints on $\mathcal{E}^\pm(k)$ are that the velocity U^\pm and energy dissipation rate ε^\pm obey

$$U^{\pm 2} = \int_{L^{-1}}^{\infty} \mathcal{E}^\pm(k) dk, \quad \varepsilon^\pm = \int_{L^{-1}}^{\infty} \nu k^2 \mathcal{E}^\pm(k) dk. \quad (\text{II.34})$$

Suppose also that $\mathcal{E}^\pm(k)$ displays an ‘‘inertial range’’ in the sense that it scales with a power of k up to the effective cut-off wavenumbers k_c^\pm . For simplicity, let us write

$$\mathcal{E}^\pm(k) = \begin{cases} A k^{-q^\pm}, & L^{-1} \leq k \leq k_c^\pm, \\ 0, & k > k_c^\pm. \end{cases} \quad (\text{II.35})$$

We also assume that k_c^\pm diverges as $\nu \rightarrow 0$, while $U^{\pm 2}$ and ε^\pm remain finite, and that A depends only upon the energy flux ε^\pm and the outer length scale $\ell = L$. Then we have the asymptotic relations

$$\varepsilon^\pm \sim \frac{U^{\pm 3}}{L} \quad \text{and} \quad L k_c^\pm \sim \left(\frac{\varepsilon^\pm}{\nu^3} \right)^{\frac{1}{9-3q^\pm}} L^{\frac{4}{9-3q^\pm}} \sim Re^{\frac{1}{3-q^\pm}}. \quad (\text{II.36})$$

Note that the scaling of k_c with Re is valid for all q^\pm and not only for Kolmogorov phenomenology (see Part IV below).

The moments of the spectrum $\langle \kappa_{n,0}^\pm \rangle_T$ satisfy

$$L \langle \kappa_{n,0}^\pm \rangle_T \sim (L k_c^\pm)^{1-\frac{q^\pm-1}{2n}} \sim Re^{\frac{1}{3-q^\pm} - \frac{1}{2n} \left(\frac{q^\pm-1}{3-q^\pm} \right)}. \quad (\text{II.37})$$

So far, this has followed the argument in Frisch [11] and Doering and Gibbon [10]. Now let us compare this scaling result with the estimate in (II.32) for $n = 2$: this correspondence tells us that

$$q^\pm \geq 3 - \frac{4}{2\lambda^\pm + \lambda^\mp} \geq \frac{5}{3}, \quad (\text{II.38})$$

with a cut-off $L k_c \sim Re^{\frac{1}{3-q^\pm}}$.

III. THE DOERING-FOIAS $Gr^\pm - Re^\pm$ RELATION FOR MHD

Following Doering and Foias [6] the forcing function $\mathbf{f}^\pm(\mathbf{x})$ is split into its magnitude F^\pm and its ‘‘shape’’ ϕ^\pm such that

$$\mathbf{f}^\pm(\mathbf{x}) = F^\pm \phi^\pm(\ell^{-1} \mathbf{x}), \quad (\text{III.1})$$

where ℓ is the longest length scale in the force. On the unit torus \mathbb{I}_d in d -dimensions, ϕ is a mean-zero, divergence-free vector field with the chosen normalization property

$$\int_{\mathbb{I}_d} |\nabla_y^{-1} \phi^\pm|^2 d^d y = 1. \quad (\text{III.2})$$

L^2 -norms of \mathbf{f}^\pm on \mathbb{I}^d are

$$\|\nabla^N \mathbf{f}^\pm\|_2^2 = C_N^\pm \ell^{-2N} L^d F^{\pm 2}, \quad (\text{III.3})$$

where the coefficients C_N^\pm refer to the shape of the force but not its magnitude

$$C_M^\pm = \sum_n |2\pi n|^{2N} |\hat{\phi}_n^\pm|^2. \quad (\text{III.4})$$

Various bounds exist such as (among others)

$$\|\nabla \Delta^{-M} \mathbf{f}^\pm\|_\infty = D_M^\pm F \ell^{2M-1}. \quad (\text{III.5})$$

The energy dissipation rate ϵ is

$$\epsilon^\pm = \left\langle \nu L^{-d} \int_{\mathcal{V}} |\nabla \mathbf{z}^\pm|^2 dV \right\rangle = \nu L^{-d} \langle H_1^\pm \rangle. \quad (\text{III.6})$$

In terms of F^\pm , the Grashof number in (II.5) becomes ($\ell = L$)

$$Gr_\pm = F^\pm \ell^3 / \nu^2. \quad (\text{III.7})$$

Following the procedure in [6] (pg 296 equation (2.9)), we multiply (II.1) by $(-\Delta^{-M})\mathbf{f}^\pm$ and integrate we obtain

$$\begin{aligned} \frac{d}{dt} \int_{\mathbb{I}_d} \mathbf{z}^\pm \cdot [(-\Delta^{-M})\mathbf{f}^\pm] dV &= \nu \int_{\mathbb{I}_d} \Delta \mathbf{z}^\pm \cdot [(-\Delta^{-M})\mathbf{f}^\pm] - \int_{\mathbb{I}_d} \mathbf{z}^\mp \cdot \nabla \mathbf{z}^\pm \cdot [(-\Delta^{-M})\mathbf{f}^\pm] dV \\ &+ \int_{\mathbb{I}_d} \mathbf{f}^\pm \cdot [(-\Delta^{-M})\mathbf{f}^\pm] dV. \end{aligned} \quad (\text{III.8})$$

Now if we integrate all the terms by parts, and take the time average, we get

$$\begin{aligned} \left\langle L^{-d} \int_{\mathbb{I}_d} |\nabla^{-M} \mathbf{f}^\pm|^2 dV \right\rangle &\leq \nu \left\langle L^{-d} \int_{\mathbb{I}_d} |\mathbf{z}^\pm \cdot (-\Delta^{-M+1})\mathbf{f}^\pm| dV \right\rangle \\ &+ \left\langle L^{-d} \int_{\mathbb{I}_d} |\mathbf{z}^\mp \cdot [\nabla[(-\Delta^{-M})\mathbf{f}]] \cdot \mathbf{z}^\pm| dV \right\rangle. \end{aligned} \quad (\text{III.9})$$

Thus, after a Schwarz inequality, (III.9) turns into

$$c_0 F^{\pm 2} \ell^{2M} \leq c_1 \nu F^\pm \ell^{2M-2} U^\pm + c_2 \ell^{2M-1} F^\pm U^\pm U^\mp. \quad (\text{III.10})$$

By using (III.7), (III.10) becomes

$$Gr_\pm \leq c (Re_\pm + Re_\pm Re_\mp), \quad Gr_\pm \rightarrow \infty. \quad (\text{III.11})$$

IV. PHENOMENOLOGICAL ARGUMENT FOR FLUIDS AND MHD

In the fluid case, the total energy and dissipation can be written in terms of the energy spectrum with spectral index q as: $U^2 = \int_{k_0}^{k_c} A k^{-q}$, $\epsilon = \nu \int_{k_0}^{k_c} A k^{2-q}$ with dimensionally $[A] = [\epsilon^a][L^b]$. One finds straightforwardly $a = 2/3$, $b = [5 - 3q]/3$, so $b = 0$ for $q = 5/3$, as expected. This leads to a cut-off wavenumber $k_c/k_0 = [\epsilon \nu^{-3}]^{1/[3(3-q)]} k_0^{-4/[3(3-q)]}$, or in terms of the Reynolds number, $Re = UL/\nu = \epsilon^{1/3} L^{4/3} \nu^{-1}$: $lk_c = Re^x$, $x = [3 - q]^{-1}$, with $\ell = 2\pi/k_0$.

In MHD, one can follow the weak-turbulence IK prescription (remaining in the isotropic framework for simplicity). Then, $A = [\epsilon B_0]^c L^d$, where B_0 is a large-scale strong (quasi)-uniform magnetic field; so $c = 1/2$, $d = [3 - 2q]/2$. This leads to $k_c/k_0 = [\epsilon B_0^{-1} \nu^{-2}]^{1/[2(3-q)]} k_0^{-3/[2(3-q)]}$ or, in terms of the Reynolds number, $Re = UL/\nu = [\epsilon B_0 L^5]^{1/4} \nu^{-1}$:

$$lk_c = r^x Re^x, \quad x = [3 - q]^{-1}, \quad r = \frac{U}{B_0} \ll 1, \quad (\text{IV.1})$$

a hypothesis that compatible with the wave-turbulence assumption. Thus, with the introduction of the factor r , the scale dependence of the cut-off wavenumber with Reynolds number is the same for fluids and MHD.

This phenomenological argument can be redone in the more general case when the velocity and magnetic fields are correlated, i.e. with $E_+ \neq E_-$. This results in a condition between the indices q_\pm of the E_\pm spectra, namely $q_+ + q_- = 3$ within the IK framework with, as before for uncorrelated flows, $q_+ = q_- = 3/2$

(see [12] for an introduction). Two-point closure computations and two-dimensional numerical simulations find $q_+ \neq q_-$ at high correlations, but the three-dimensional case remains open. As in the preceding case of uncorrected MHD, we make the assumption that the \pm integral scales are both comparable to the box size ℓ .

After some algebra along the same lines as before, one finds that the dissipative wave numbers for the $E_{\pm}(k)$ spectra are equal both to $k_+ = k_- = k_c = \epsilon/[\nu^2 B_0]^{1/3}$, as in the zero-correlation case, or:

$$\ell k_{\nu} = [z_0^+/B_0]^{1/3} [z_0^-/B_0]^{1/3} Re_+^{1/3} Re_-^{1/3}, \quad (\text{IV.2})$$

with $Re_{\pm} = z_0^{\pm} \ell / \nu$, having assumed that the magnetic Prandtl number is equal to unity so that $\nu = \eta = \nu_+ = \nu_-$. Writing

$$E_{\pm}(k) = A_{\pm}(\epsilon, B_0, \ell) k^{-q_{\pm}}, \quad A_{\pm}(\epsilon, B_0, \ell) = \epsilon^{a_{\pm}} B_0^{b_{\pm}} \ell^{c_{\pm}}, \quad (\text{IV.3})$$

it is readily found that, under the assumption that $b_+ + b_- = -3(a_+ + a_-) + 4 = 1$ (so that $E_+(k)E_-(k) \sim [\epsilon B_0] k^{-3}$), and that $c_+ + c_- = -3 + (3 - q_+) + (3 - q_-)$. Then:

$$\ell k_c \sim \frac{\epsilon}{[\nu^2 B_0]} \frac{1}{(3-q_+)+(3-q_-)} \ell \frac{3}{(3-q_+)+(3-q_-)}, \quad (\text{IV.4})$$

or in terms of Reynolds numbers:

$$\ell k_c \sim [[z_0^+/B_0][z_0^-/B_0]]^{\frac{1}{(3-q_+)+(3-q_-)}} [Re_+ Re_-]^{\frac{1}{(3-q_+)+(3-q_-)}}. \quad (\text{IV.5})$$

Finally, this phenomenological relation can be used as in the non-correlated case to establish the upper bounds of spectral indices. In this case one finds that:

$$\frac{1}{(3-q_+)+(3-q_-)} \left[1 - \frac{q_+ - 1}{4} \right] \leq \min \left\{ \frac{\lambda_+ + 1}{4}; \frac{\lambda_-}{8} \right\}, \quad (\text{IV.6})$$

and similarly

$$\frac{1}{(3-q_+)+(3-q_-)} \left[1 - \frac{q_- - 1}{4} \right] \leq \min \left\{ \frac{\lambda_- + 1}{4}; \frac{\lambda_+}{8} \right\}, \quad (\text{IV.7})$$

with $1 < q_{\pm} < 3$ and $1 + \lambda_{\pm}/2 < 2$ using equation (II.20). These results are to be contrasted to the uncorrelated case (see equations (II.36, II.37)) obtained in the Kolmogorov framework. It is possible to show that in the correlated case the IK spectrum $q_{\pm} = 3/2$ cannot be excluded.

V. VORTICITY AND CURRENT EQUATIONS

We have used the following four identities for vectors \mathbf{D} and \mathbf{G} , not necessarily divergence-free:

$$\nabla \times [\nabla \times \mathbf{D}] = \nabla[\nabla \cdot \mathbf{D}] - \nabla^2 \mathbf{D}, \quad (\text{V.1})$$

$$\nabla[\mathbf{D} \cdot \mathbf{Q}] = \mathbf{D} \times [\nabla \times \mathbf{Q}] + \mathbf{Q} \times [\nabla \times \mathbf{D}] + \mathbf{D} \cdot \nabla \mathbf{Q} + \mathbf{Q} \cdot \nabla \mathbf{D}, \quad (\text{V.2})$$

$$\nabla \cdot [\mathbf{D} \times \mathbf{Q}] = \mathbf{Q} \cdot \nabla \times \mathbf{D} - \mathbf{D} \cdot \nabla \times \mathbf{Q}, \quad (\text{V.3})$$

$$\nabla \times [\mathbf{D} \times \mathbf{Q}] = \mathbf{Q} \cdot \nabla \mathbf{D} - \mathbf{D} \cdot \nabla \mathbf{Q}. \quad (\text{V.4})$$

The equation for the vorticity is derived rather straightforwardly:

$$\partial_t \boldsymbol{\omega} + \mathbf{u} \cdot \nabla \boldsymbol{\omega} = \boldsymbol{\omega} \cdot \nabla \mathbf{u} + \mathbf{b} \cdot \nabla \mathbf{j} - \mathbf{j} \cdot \nabla \mathbf{b}. \quad (\text{V.5})$$

By using $\mathbf{D} = \mathbf{u} \times \mathbf{b}$ in the above identities (with $\nabla \cdot \mathbf{D} \neq 0$), we obtain the equation for the current:

$$\partial_t \mathbf{j} = \nabla[\nabla \cdot [\mathbf{u} \times \mathbf{b}] - \nabla^2 [\mathbf{u} \times \mathbf{b}]], \quad (\text{V.6})$$

which, upon expansion, leads to:

$$\nabla[\nabla \cdot [\mathbf{u} \times \mathbf{b}]] = \boldsymbol{\omega} \cdot \nabla \mathbf{b} + \mathbf{b} \cdot \nabla \boldsymbol{\omega} - \mathbf{b} \times \nabla^2 \mathbf{u} + \boldsymbol{\omega} \times \mathbf{j} - \mathbf{u} \cdot \nabla \mathbf{j} - \mathbf{j} \cdot \nabla \mathbf{u} + \mathbf{u} \times \nabla^2 \mathbf{b} - \mathbf{j} \times \boldsymbol{\omega} \quad , \quad (\text{V.7})$$

$$-\nabla^2[\mathbf{u} \times \mathbf{b}] = -\nabla^2 \mathbf{u} \times \mathbf{b} - \mathbf{u} \times \nabla^2 \mathbf{b} - 2\Sigma_i \partial_i \mathbf{u} \times \partial_i \mathbf{b} \quad . \quad (\text{V.8})$$

So the equation for the current (note the cancellations in the ∇^2 terms) is:

$$\partial_t \mathbf{j} + \mathbf{u} \cdot \nabla \mathbf{j} - \boldsymbol{\omega} \cdot \nabla \mathbf{b} - \mathbf{b} \cdot \nabla \boldsymbol{\omega} + \mathbf{j} \cdot \nabla \mathbf{u} - 2\boldsymbol{\omega} \times \mathbf{j} = -2\Sigma_i \partial_i \mathbf{u} \times \partial_i \mathbf{b} \quad , \quad (\text{V.9})$$

an expression already written in [12]. For the curl of the Elsässer field $\boldsymbol{\omega}^+ = \boldsymbol{\omega} + \mathbf{j}$, we have (with \pm symmetry for $\partial_t \boldsymbol{\omega}^-$):

$$\partial_t \boldsymbol{\omega}^+ + \mathbf{z}^- \cdot \nabla \boldsymbol{\omega}^+ = \boldsymbol{\omega}^- \cdot \nabla \mathbf{z}^+ + \boldsymbol{\omega}^- \times \boldsymbol{\omega}^+ + \Sigma_i \partial_i \mathbf{z}^+ \times \partial_i \mathbf{z}^- \quad (\text{V.10})$$

Note that the geometry term $2\boldsymbol{\omega} \times \mathbf{j}$ in the equation for the current density does not appear in the vorticity equation; also, it is weak for almost-aligned current and vorticity (or $\boldsymbol{\omega}^\pm$) [1, 13]. The equations (V.10) for the temporal evolution of $\boldsymbol{\omega}^\pm$ follow immediately from the above. Note that $\boldsymbol{\omega}^- \times \boldsymbol{\omega}^+ = 2\boldsymbol{\omega} \times \mathbf{j}$ does not affect the point-wise production of $\boldsymbol{\omega}^\pm$, whereas the second term can create current density; here the labels $i = 1, 2$, and 3 refer respectively to the x, y , and z derivatives. Finally note that, for a flow evolving towards strong local correlations between the velocity and magnetic field ($\mathbf{z}^+ = 0$ or $\mathbf{z}^- = 0$), this extra term is weak.

- [1] J. Stawarz, A. Pouquet, and M.-E. Brachet, Phys. Rev. E **86**, 036307 (2012).
- [2] B. Bigot, S. Galtier, and H. Politano, Phys. Rev. E **78**, 066301 (2008).
- [3] H. Homann, Y. Ponty, G. Krstulovic, and R. Grauer, New J. Phys. **16**, 075014 (2014).
- [4] G. Krstulovic, M.-E. Brachet, and A. Pouquet, Phys. Rev. E **89**, 043017 (2014).
- [5] G. Sahoo, P. Perlekar, and R. Pandit, New J. Physics **13**, 013036 (2011).
- [6] C. R. Doering and C. Foias, J. Fluid Mech. **467**, 289 (2002).
- [7] D. Donzis, J. Gibbon, A. Gupta, R. Kerr, R. Pandit, and D. Vincenzi, J. Fluid Mech. **732**, 316 (2013).
- [8] J. Gibbon, D. Donzis, A. Gupta, R. Kerr, R. Pandit, and D. Vincenzi, Nonlinearity **27**, 2605 (2014).
- [9] J. Gibbon, Comm Math. Sci **10**, No **1**, 131 (2011).
- [10] C. R. Doering and J. D. Gibbon, Physica D **165**, 163 (2002).
- [11] U. Frisch, *Turbulence: The Legacy of A. N. Kolmogorov* (Cambridge University Press, Cambridge, 1995).
- [12] A. Pouquet, in *Vth European School in Astrophysics, San Miniato; Lecture Notes in Physics "Plasma Astrophysics" vol. 468*, edited by C. Chiuderi and G. Einaudi (Springer-Verlag, 1996), pp. 163–212.
- [13] S. Servidio, W. Matthaeus, M. Shay, P. Cassak, and P. Dmitruk, Phys. Rev. Lett **102**, 115003 (2009).
- [14] At $m = 1$, we have equality with $c_1 = 1$. The case $m = \infty$ needs a logarithmic correction.
- [15] The simple Hölder inequality $\Omega_1^\pm \leq \Omega_m^\pm$ translates to $D_1^{\pm\alpha_m/2} \leq D_m^\pm$ which, in turn, implies that $\lambda^\pm \geq 1$.
- [16] For technical reasons, as shown in [10], an additive term should be included in both the denominator and numerator in (II.21) to take account of the forcing term in (II.16), but as this makes a negligible contribution it will be dropped.
- [17] As a check we note that if $\chi_{m,\lambda}^+ = \chi_{m,\lambda}^- = m\lambda + 1 - \lambda$, as it does in the pure 3D Navier-Stokes case [8], then the sum of the exponents on the right hand side of (II.22) is $\frac{1}{2}\lambda$, as it should.